AD-A205 193 ELECTRON DENSITY PROFILES AND PLASMA DRIFT MEASUREMENTS 1/1
WITH DIGITAL IONOSONDES(U) LOWELL UNIV MA CENTER FOR
ATMOSPHERIC RESEARCH B W REINISCH ET AL. SEP 88
UNCLASSIFIED ULRF-442/CAR AFGL-TR-88-0233 F/G 4/1 NL

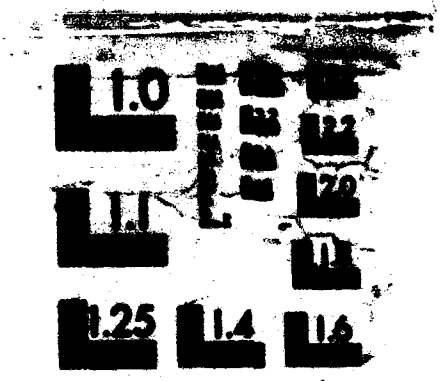
1.0
1.1
1.25
1.4
1.6

UNCLASSIFIED

SECURITY CLASSIFICATION OF THIS PAGE

REPORT DOCUMENTATION PAGE

Form Approved OMB No. 0704-0188

1a. REPORT SECURITY CLASSIFICATION: Unclassified	1b. RESTRICTIVE MARKINGS: N/A
2a. SECURITY CLASSIFICATION AUTHORITY: N/A	3. DISTRIBUTION/AVAILABILITY OF REPORT: Approved for public release; distribution unlimited.
2b. DECLASSIFICATION/DOWNGRADING SCHEDULE: N/A	
4. PERFORMING ORGANIZATION REPORT NUMBER(S): ULRF 442/CAR	5. MONITORING ORGANIZATION REPORT NUMBER(S): AFGL-TR-88-0233
6a. NAME OF PERFORMING ORGANIZATION: University of Lowell, Center for Atmospheric Research	6b. OFFICE SYMBOL (If applicable):
6c. ADDRESS (City, State, and ZIP Code): 450 Aiken Street, Lowell, Massachusetts 01854	7a. NAME OF MONITORING ORGANIZATION: Air Force Geophysics Laboratory
7b. ADDRESS (City, State, and ZIP Code): AFGL/LIS, Hanscom AFB, MA 01731	
8a. NAME OF FUNDING/SPONSORING ORGANIZATION: Air Force Geophysics Laboratory	8b. OFFICE SYMBOL (If applicable): AFGL/LIS
8c. ADDRESS (City, State, and ZIP Code): AFGL/LIS, Hanscom AFB, MA 01731	9. PROCUREMENT INSTRUMENT IDENTIFICATION NUMBER: F19628-86-K-0036
	10. SOURCE OF FUNDING NUMBERS: PROGRAM ELEMENT NO. 62101F; PROJECT NO. 4643; TASK NO. 08; WORK UNIT ACCESSION NO. AJ

11. TITLE (Include Security Classification): Electron Density Profiles and Plasma Drift Measurements with Digital Ionosondes

12. PERSONAL AUTHOR(S): Bodo W. Reinisch, Jurgen Buchau,* Robert R. Gamache, Klaus Bibl, Gary S. Sales, Ivana Stanisla,** Lee F. Mollenkopf***

13a. TYPE OF REPORT	13b. TIME COVERED	14. DATE OF REPORT (Year, Month, Day)	15. PAGE COUNT
Scientific Report No. 2	FROM July '87 TO June '88	1988, September	32

16. SUPPLEMENTARY NOTATION: AFGL/LIS, Hanscom AFB, MA 01731, *Heinrich Institute of Radiowave Propagation, P.O. Box 138, Xinxiang, Henan, PRC, **Andrew Antennas, Innovation House, Technology Park, The Levels, S.A. 5095, Australia

17. COSATI CODES: FIELD	GROUP	SUB-GROUP

18. SUBJECT TERMS (Continue on reverse if necessary and identify by block number): Ionospheric; Electron Density Profiles; Digital Ionosonde; Ionospheric Drift, Tilt and Roughness. 40, 10

19. ABSTRACT (Continue on reverse if necessary and identify by block number):

Knowledge of the three dimensional electron density distribution and the plasma drift in the earth's ionosphere is needed for the radio communication engineer and the geophysicist. The combination of global models, e.g. the International Reference Ionosphere (IRI), modern digital ionosondes, and relatively powerful micro-computers provide the capabilities to overcome the limitations that have heretofore prevented real time ionospheric specification and improved forecasting techniques. The developing network of digital ionosondes provides an improved ionogram data set. The cumbersome evaluation of electron density profiles (EDP), from the ionograms, has been eased with automatic ionogram scaling and related micro-computer based algorithms for calculating EDPs.

The purpose of this Scientific Report is to summarize the evolving network of digital ionosondes based on the Digisonde 256 technology and to present techniques that have been developed for calculating electron density profiles and determining the drift velocities.

(Continued)

20. DISTRIBUTION/AVAILABILITY OF ABSTRACT: UNCLASSIFIED/UNLIMITED ☐ SAME AS RPT. ☐ DTIC USERS	21. ABSTRACT SECURITY CLASSIFICATION: Unclassified
22a. NAME OF RESPONSIBLE INDIVIDUAL: Jeffrey H. Thompson	22b. TELEPHONE (Include Area Code): 617-377-3061
	22c. OFFICE SYMBOL: AFGL/LIS

DD Form 1473, JUN 86 — Previous editions are obsolete.

SECURITY CLASSIFICATION OF THIS PAGE

UNCLASSIFIED

UNCLASSIFIED

19. ABSTRACT (Continued)

In addition, examples are presented to illustrate relevant data processes that can be developed and utilized to the needs of the communication or radar system manager and to the needs of the geophysicist involved in basic and applied research in solar-terrestrial physics. keywords: → to field 18

UNCLASSIFIED

TABLE OF CONTENTS

FOREWORD

Within several years, a worldwide network of approximately 40 digital ionosondes will be operating to further understanding of solar-terrestrial and radio physics. The digital ionosondes possess capabilities to provide data bases that heretofore were limited to instruments requiring a significant capital investment (e.g. incoherent scatter radar) or were labor intensive to obtain (e.g. real-height analyses).

With the maturation of the Digisonde hardware, there has been associated analytical work to develop automatic, micro-computer based algorithms that will provide reliable data bases of the aforementioned types.

The University of Lowell Center for Atmospheric Research, with cooperation and support from the Air Force Geophysics Laboratory recently contributed three papers that document the planned digital ionosonde network and the approaches and results of the associated analytical investigations.

The first paper summarizes the global Digisonde 256 network, the ionogram and drift operating modes and the resulting data. The drift mode of operation, in addition to determining the mean ionospheric motion within the instrument's field-of-view, provides high resolution Doppler spectra of the signals obtained from seven spaced receiving antennas. These data can be used to determine ionospheric tilts and roughness. Data editing and processing programs have been developed to present, on a single page, ionospheric characteristics and ionogram surveys. These examples serve as a base for defining data handling and archival formats that can result from these improved, contemporary data sets. The

examples are shown to illustrate how the resulting data may be summarized and presented to benefit the radio communications engineer and the geophysicist.

The second paper summarizes the techniques developed by the University of Lowell Center for Atmospheric Research (ULCAR) group to determine the true height electron density profile from the virtual height ionogram trace. The ULCAR technique is based on a sum of the shifted Chebyshev polynomials that represents the true height for each ionospheric layer. The methods for determining the ionospheric profile starting height and the conditions for joining the layers are discussed in this paper. A comparison is made of the ULCAR and POLAN (Chapman profile shape) profiling methods. An analysis of 172 ionograms reveals an average height difference of -2.0 kilometers and a mean peak height difference of +7.6km. Given electron density profiles, a comparison is made of the Dudney ionospheric model heights of the F2 layer as a function of the ratio of foF2 to foE. It was found that the Dudney model yields systematically high height values for daytime and low height values for nighttime. It is suggested that these systematic differences may result from the model's neglect of underlying ionization or a variation of the F2 region scale height with altitude. The modern ionosonde produces important data for understanding ionospheric phenomena and for the development of improved ionospheric models. The utility of these modern data is not limited by the storage media, and new opportunities are opening for tailored data presentation, analysis and archival consistent with the needs of the application and research communities.

The third paper discusses an alternative representation of the F2 region electron density profile. The ULCAR Chebyshev polynominal requires five coefficients plus the beginning and ending frequencies of the layer. In the POLAN single-polynominal mode, 11 parameters are needed to represent the F2 electron density profile. The LAY function, defined by four parameters [foF2, Hmax (peak height), HX (height parameter) and SC (scale parameter)], may lend itself to improved real time processing. Three thousand electron density profiles calculated from the POLAN fourth order polynomial expansion were compared to the profiles determined using the LAY function. The comparison shows that for most of the time the LAY functions, with five kilometer maximum error, represent the F2 layer down to f = foE or foF1 during the day and to the first scaled ionogram frequency during the night. It was also found that the LAY function parameters (HX/Hmax and SC) have fairly small diurnal variations in their median values. This study could be expanded to represent the entire electron density profile as a linear combination of LAY functions and to investigate the behavior of the associated LAY parameters.

This scientific report includes the recent papers mentioned above:

Reinisch, B. W., J. Buchau, K. Bibl and G. S. Sales, "Multistation/Multiparameter Observations with a Network of Digital Ionosondes," invited paper presented to the Electromagnetic Wave Propagation Panel, North Atlantic Treaty Organization, Advisory Group for Aerospace Research and Development, Munich, Federal Republic of Germany, May 1988. Proceedings forthcoming.

Reinisch, B. W., R. R. Gamache, H. Xueqin and L. F. McNamara, "Real Time Electron Density Profiles from Ionograms," Advances in Space Research, Ionospheric Informatics, 8, 4, (4)63-(4)72, 1988.

Bossy, L., R. R. Gamache and B. W. Reinisch, "LAY-Functions for F2 Profiles," Advances in Space Research, Ionospheric Informatics, 8, 4, (4)201-(4)204.

MULTISTATION/MULTIPARAMETER OBSERVATIONS WITH A NETWORK OF DIGITAL IONOSONDES

R. W. Reinisch,[1] J. Buchau,[2] K. Bibl[1] and G. S. Sales[1]

(1) University of Lowell Center for Atmospheric Research, Lowell, MA 01854, U.S.A.
(2) Air Force Geophysics Laboratory, Hanscom AFB, MA 01731, U.S.A.

Summary

The global network of modern ionosondes generates a data set of ionospheric characteristics that can serve as test bed for the developing ionospheric models. Remote access to each station makes it possible to use real time data for project planning and radio communication tasks. Real ionospheric parameters like ionospheric roughness, tilt angles and drift are now available for each Digisonde location.

1. Introduction

A new generation of modern ionosondes is now being deployed world-wide. By the end of 1990, a network of some forty of these ionosondes (Reinisch, 1986) will provide a consistent data set of ionospheric parameters that are automatically scaled in real time. The automated stations output the standard ionospheric parameters, the h'(f) traces with amplitudes and Doppler frequencies, and the electron density profiles. All these data can be remotely accessed by telephone links, and they are, in general, archived on half-inch magnetic tape.

New measuring techniques make it possible to determine ionospheric structure and dynamics in a more or less routine way. After completion of an ionogram, the sounder measures ionospheric drift and structure using high resolution Doppler shift and incidence angle observations. High latitude drift observations monitor the polar cap convection pattern, and first results from Millstone Hill (42.6°N, 71.5°W) show that this pattern can also control the drift at this mid-latitude location. F-layer tilts, measured at mid-latitude, show typical tilt angles of 2 to 5°; values of 10° are observed occasionally. Observations of the smoothness of the mid-latitude F-layer, as defined by the inverse of the size of the reflection area, show a characteristic day/night variation. During the day the echoes arrive within a small angular cone of $\theta < 5°$ (smooth ionosphere), while this angle increases to some 20° at night (rough ionosphere).

2. Digisonde Network

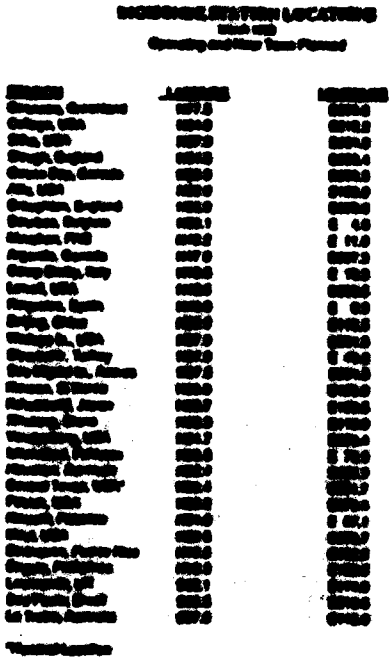

Table 1

There are currently 32 Digisonde 256 systems (Table 1) in operation or are close to being installed. The global station distribution, as shown in Figure 1, is very uneven, the majority of sites lying in the northern hemisphere, and there are no equatorial stations. Nevertheless this network provides an extensive data base of ionospheric parameters in digital form, making it easy to process and analyze the data in terms of average diurnal variations, storms, and irregularities. This data base will be invaluable for the testing of global ionosphere models.

The scaled ionogram parameters and/or the raw ionograms can be remotely accessed via voice grade telephone links operating at 1200 or 2400 baud. Currently only the U.S. Global Air Weather Service is networking in a real time mode by polling all their Digisondes and centrally collecting the ionospheric parameters as soon as an ionogram scan and the 20 to 30 second ARTIST processing is completed. In general, all stations record the raw ionograms and the autoscaled data on half-inch magnetic tape (1600 bpi).

By adding transmit antennas for oblique transmissions to the stations the Digisondes can be used to record oblique digital ionograms (Reinisch et al., 1988, Anand et al., 1986). A project is underway to automate both operation and scaling for oblique ionograms, thus adding more sampling points to the global data set.

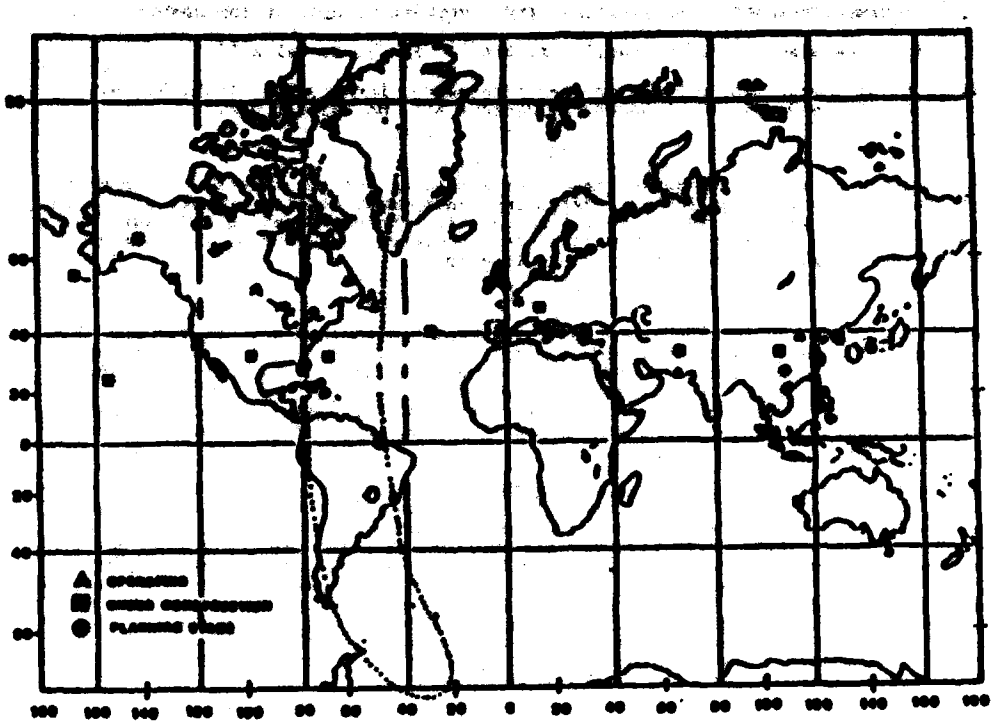

GLOBAL DIGISONDE 256 NETWORK

Figure 1

3. Ionospheric Data

The Digisonde 256 has three basic modes of operation: (1) vertical incidence ionograms, (2) drift observations, and (3) oblique incidence (bistatic) ionograms. Since the third mode is not yet fully automated and the necessary processing software is not yet developed, we limit the discussion to modes 1 and 2.

3.1 Ionogram Characteristics

The Digisonde scales the ionograms within 20 to 30 seconds after completion of the ionogram scan using the ARTIST routine (Reinisch and Huang, 1983). Figure 2 is an example of a typical on-line printout from the University of Lowell station at Millstone Hill in Westford, MA (42.6°N, 71.5°W geogr.). The small numbers using optically weighted font Petencsdy et al., 1973) give the amplitudes in multiples of 4 dB for the vertical incidence echoes with ordinary polarization, the X indicates extraordinary polarization, and the arrows point to the direction from where oblique echoes are received. The arrows composing the E region at 120 km all point to the north-east. The oblique F echoes between 4.5 and 6.5 MHz come from the south and southeast. ARTIST finds the leading edge of the overhead echo traces for the E and F layers. The autoscaled h'(f) traces, marked by the letters E and F, are superimposed on the raw ionogram, thus providing a means of checking the ARTIST performance. The letter T is used for presenting the calculated true height profile. For each layer, E, F1 and F2, the profile is given in terms of a modified sum of Chebyshev polynomials (Bennett et al., 1976). The coefficients of the Chebyshev polynomials are stored on magnetic tape and transmitted to the data center via telephone links. ARTIST scales the following ionogram parameters: foF2, foF1, foE, foEs, MUF3(3000), fmin, fmin, h'F, h'F2, h'E and h'Es. The frequency spread for both E and F is determined, and also the average range spread (listed as FE, FF, QE and QF in Figure 2). The virtual height traces h'(f)E and h'(f)F are recorded together with the measured echo amplitudes and Doppler frequencies.

Is the quality of the autoscaled data adequate for the high frequency radio communication and radar engineers, and for the ionospheric modelers? Recent comparisons of ARTIST scalings for foF2 and MUF(3000) with manual readings by experienced ionogram scalers (Gilbert and Smith, 1986) show that ARTIST provides acceptable values for about 93% of the time at a mid-latitude station. For 97% of the analyzed ionograms, foF2 was determined within ±0.5 MHz. This is somewhat better than the 87% (Reinisch and Huang, 1983) found for the auroral station at Goose Bay (54.6°N CGM).

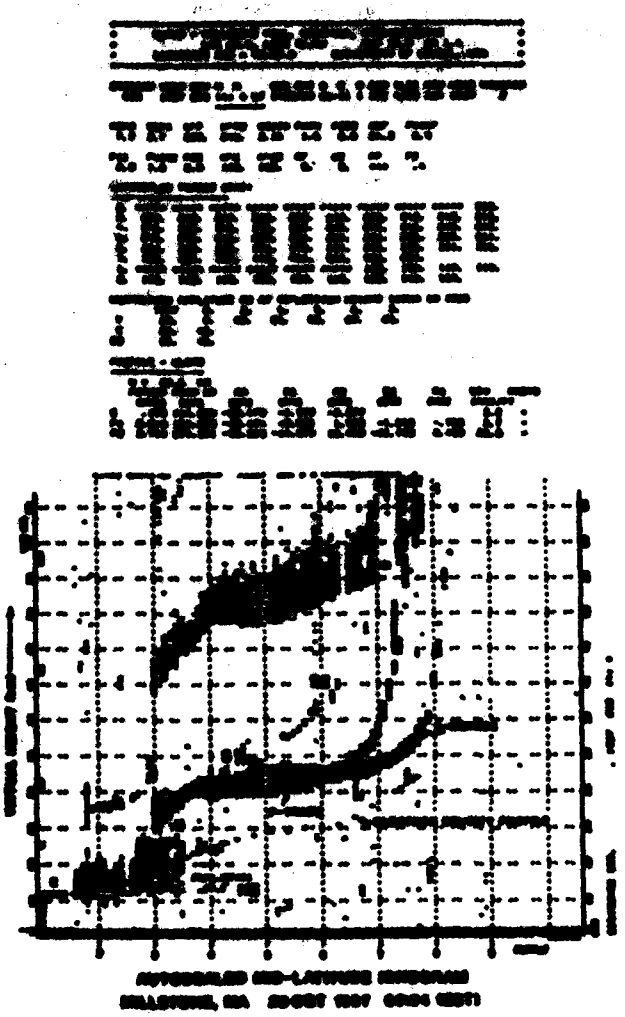

Figure 2

The WLCAR group has recently developed the ARTIST Data Editing Program (ADEP) to establish a quality control for the ARTIST data. Inconsistent values are automatically detected, the raw ionogram together with the ARTIST traces are displayed on a computer display screen, and an operator can make the required corrections. The electron density profiles are updated automatically. The edited ARTIST data are then recorded on a 1.2 Mbyte floppy disk which can store the characteristics for about 1,700 ionograms. This floppy disk will be the form in which the data of the WLCAR station will be published, containing much more information than is normally published by ionospheric stations. Besides the standard ionospheric parameters the disk contains the echo traces, i.e. h'(f), the echo amplitudes and Doppler frequencies and the coefficients for the calculation of the electron density profiles.

A companion program to ADEP prints frequency plots and electron density contours, as shown in Figure 3, displaying the data for 10 October 1987 at Millstone. foE, foEs, foF1 and foF2 are plotted in the top panel. The extent of the frequency spread of the

F trace is indicated on the foF2 curve. The lower half of the figure shows the height variations for given electron densities (plotted as plasma frequency contours in 0.5 MHz increments); the top curve is hmF2. Local midnight and noon are marked by M and N, and sunrise and sunset is marked by an F and an E for the F and E region, respectively. It is proposed that this display become the standard presentation for the data from the Digisonde network. For specific case studies it may be useful to review the original ionograms. The ionogram survey (Figure 4) displays the 96 quarter hour ionograms for one day on a single page. Only overhead echoes with ordinary polarization are printed, oblique and X polarization echoes are deleted.

3.2 Drift Mode Data

In the drift mode, the Digisonde determines high resolution Doppler spectra for each of the signals received on seven spaced receiving antennas (Reinisch et al., 1987, Buchau et al., 1987). The incidence angle of each spectral signal component is calculated from the seven respective phases, resulting in a skymap that shows the location of the simultaneously existing reflection points (sources) and their respective Doppler frequencies. Tight clustering of the sources indicates a smooth ionosphere, wide spread a rough ionosphere. We defined a roughness index RI that is proportional to the angular extent of the source region. Figure 5 shows this index for Erie, CO, during a disturbed period in March and a quiet period in April. The solar zenith angle is plotted on tops of the figure. The roughness index of 2 at noon indicates an angular size of the reflection area of about 10°, while RI = 12 at night during the disturbed period indicates 60°. This pattern of smooth daytime and rough nighttime contours was seen on all the Colorado data and also on data from the subauroral station at Argentia, Newfoundland (Figure 6). The night RI increases with increasing magnetic activity as illustrated in Figures 5 and 6.

This center of gravity of the source locations defines the tilt vector consisting of a tilt angle, measured from the overhead position, and tilt direction, measured clockwise from true north. The diurnal variation of these two parameters for Erie, CO is shown in Figure 7 for 5/6 March 1988. These tilt parameters are well defined only when the ionospheric roughness is small. There is a large uncertainty in defining the tilt parameters when the sources are spread over the sky. Figure 7 indicates a consistent southward tilt increasing from 2° to 3° during the daytime. Large angles of up to 10° are occasionally observed.

When the sources are sufficiently spread the three-dimensional drift velocity vector which best reproduces the observed Doppler frequencies (Dennis, 1983) is calculated. In general, we assume a uniform plasma velocity over the entire skymap (zenith angle $\theta < 90°$). Routine observations in the polar cap and the auroral regions (Buchau et al., 1987) show the predominantly antisunward plasma convection for long periods of time.

The F region drift in the central polar cap (Qanaq, Greenland, 87.6°W CGL) is shown for five consecutive days, October 18 to 22, 1987 in Figure 8. Direction and magnitude of the horizontal drift vector are plotted against universal time. For a southward z component of the interplanetary magnetic field (IMF) one expects an antisunward drift (Cauffman et al., 1977). Since the IMF data were not available for the period covered in Figure 8 we listed the Kp values. As seen here and also in other data, the drift direction is generally antisunward when Kp ≥ 2 while strong deviations in the sunward direction are observed when Kp is very small. In the period covered by Figure 8, the most consistent antisunward convection occurs from 13 UT on 20 October to 21 UT on the next day, when Kp varies between 2 and 4. A 90° deviation is observed from midnight to 12 UT on 20 October. October 22 shows sunward convection for about 8 hours starting at 12 UT when Kp = 1. The Qanaq ionogram survey (vertical O trace only) for 20 October (Figure 9) reveals that the F region was disturbed until 12 UT, and the F traces show spreading and forking. After 13 UT, when the drift is consistently antisunward, the ionogram signatures are different, suggesting a fairly smooth ionosphere, even though Kp increases to 4.

4. Conclusions

The growing Digisonde 256 network makes it possible for the first time to obtain electron density profiles of the bottomside ionosphere on a global basis with good time resolution. All the data reduction is done in real time leaving only data editing and display to be done off line. It seems that this data base can provide the test bed for the ionospheric modeling efforts. A world-wide study of the ionospheric roughness and the ionospheric drift could give new inputs to the modelers. It will be important to conduct coordinated measuring campaigns to study large scale phenomena like atmospheric gravity waves.

Acknowledgement

This work was in part supported by the University of Lowell and in part by the Air Force Geophysics Laboratory, Hanscom AFB, Massachusetts.

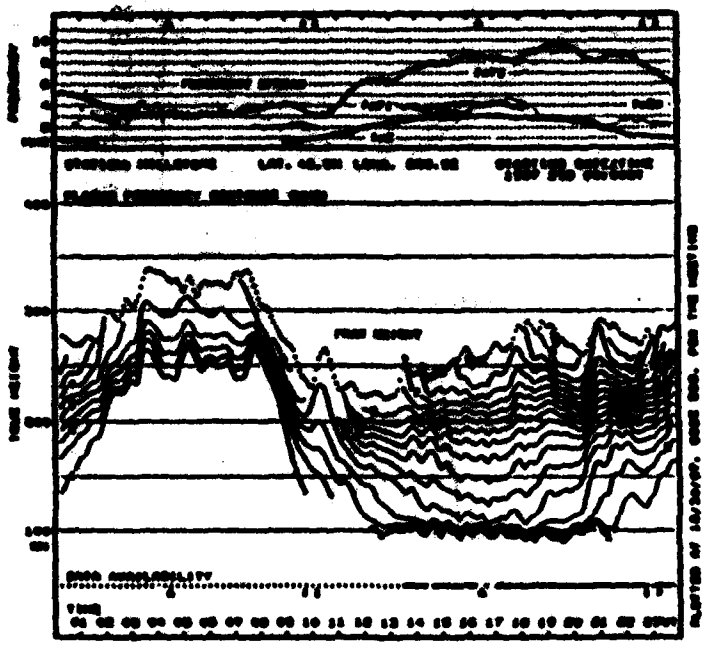

IONOSPHERIC CHARACTERISTICS
MILLSTONE, MA 20 OCT 987

Figure 3

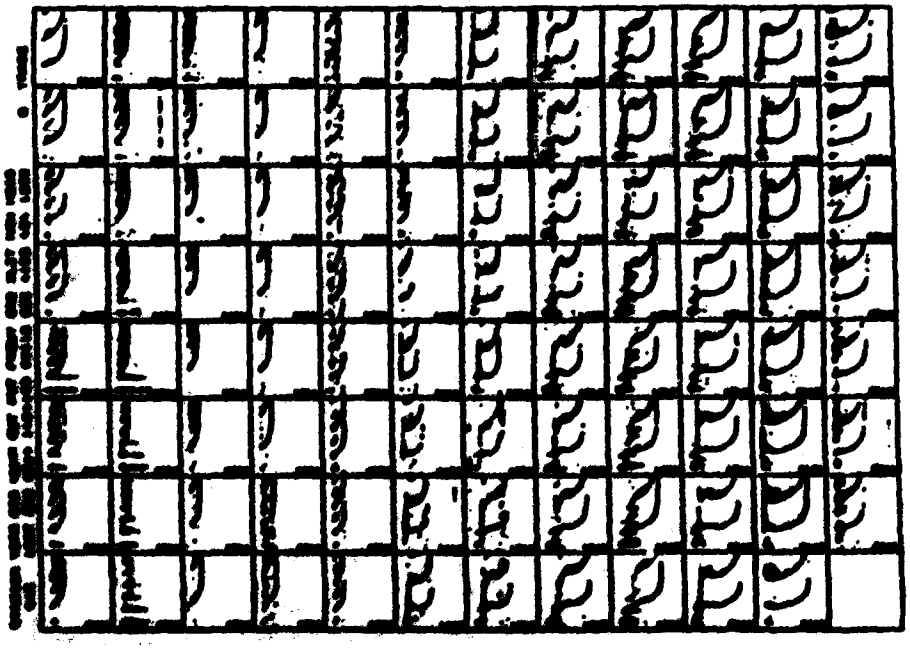

IONOGRAM SURVEY (X Trace and Oblique Signals Suppressed)
MILLSTONE, MA 20 OCT 1987

Figure 4

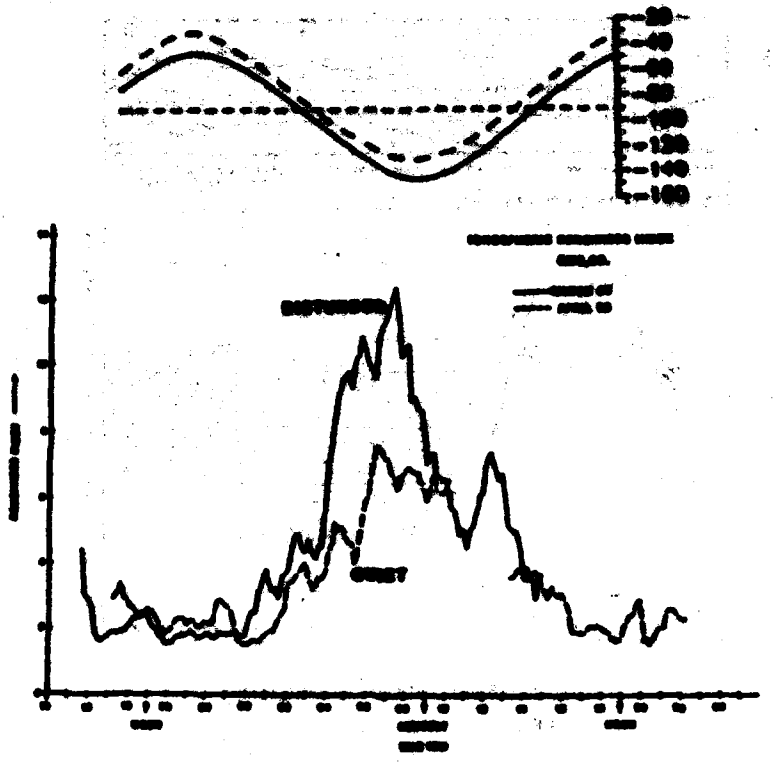

DIURNAL VARIATION OF ROUGHNESS INDEX

Figure 8

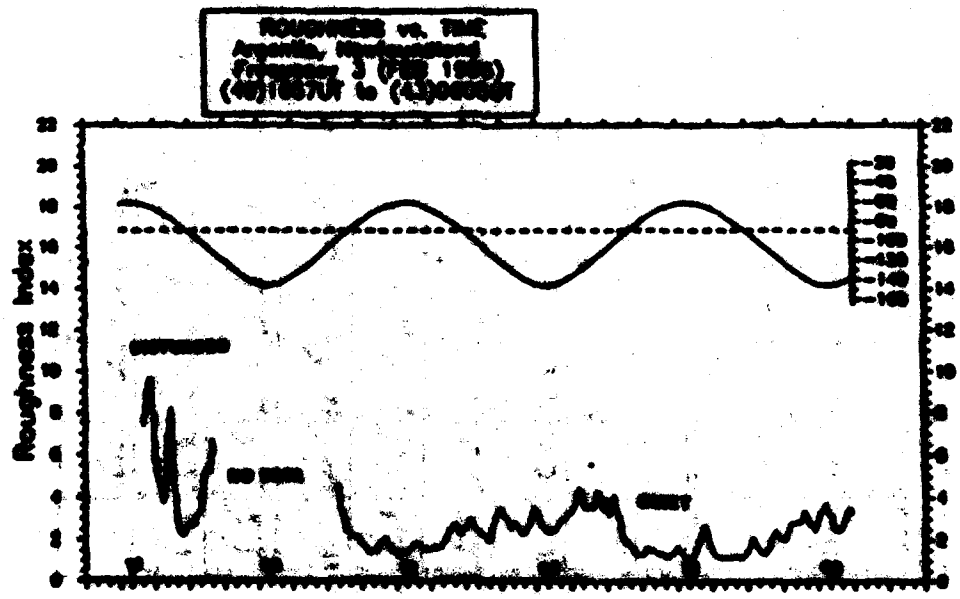

Figure 9

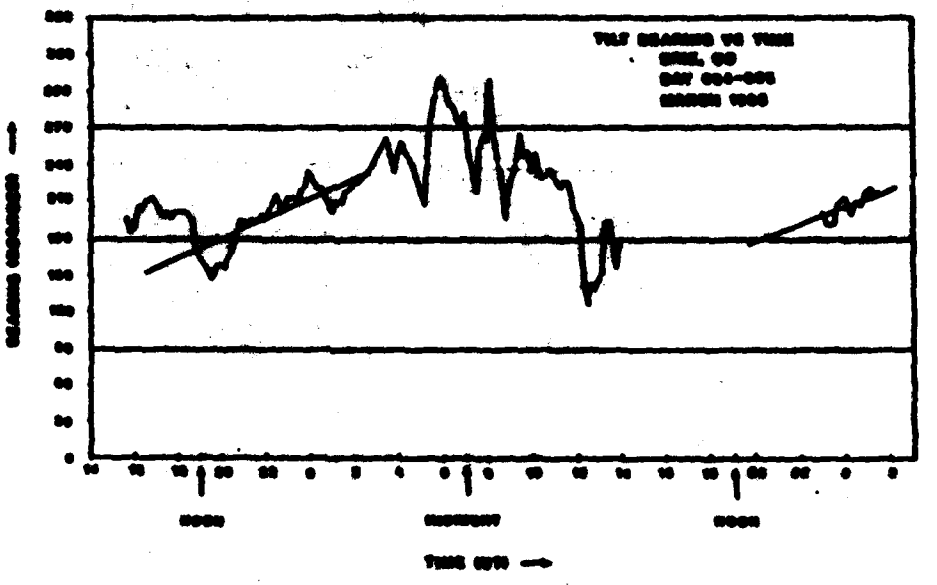

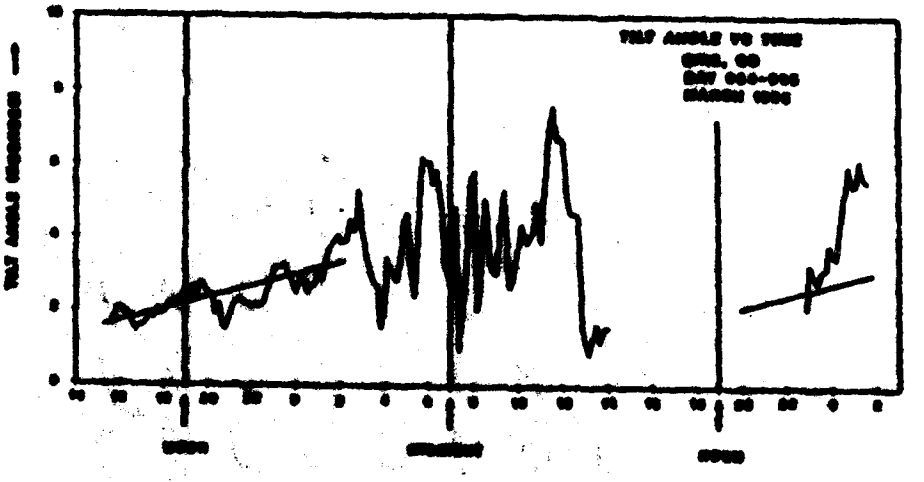

Figure 7

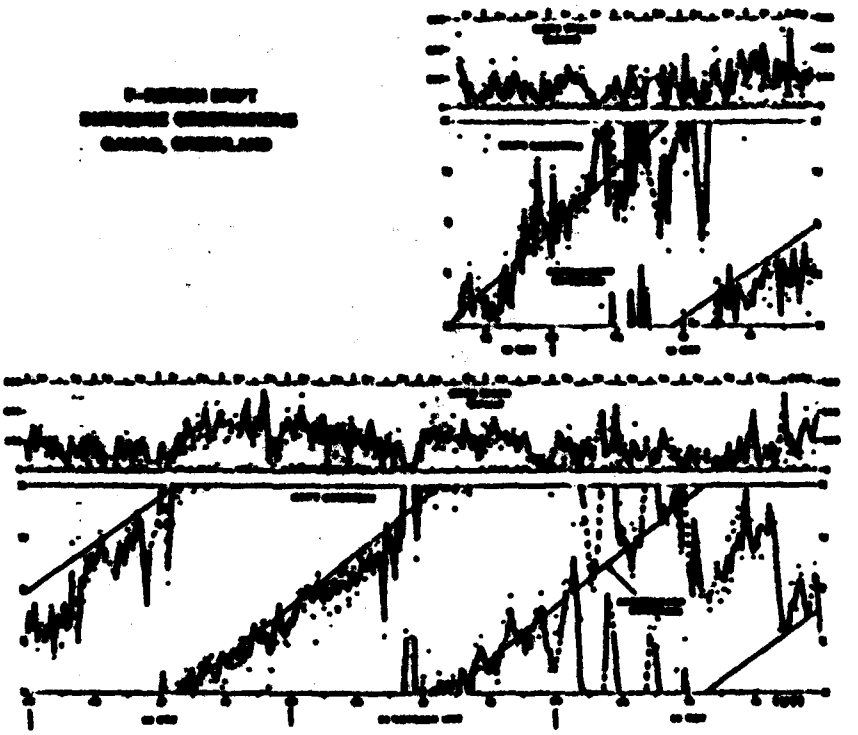

Figure 8

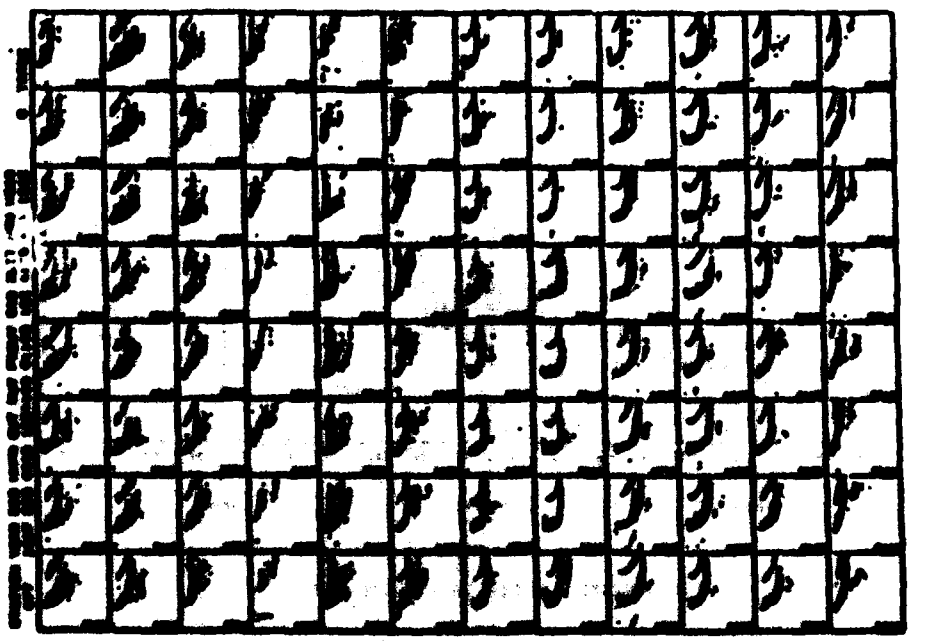

Figure 9

Ahmad, N., G. S. Sales and R. W. Reinisch, "Frequency Management of a Long Range HF Communication Link Using Ionospheric Data," Proceedings of the IEEE MILCOM Conference, pp. 209-213, October 20-23, 1985.

Bushuev, J., R. W. Reinisch, R. R. Anderson, E. J. Weber and C. Beaulieu, "Polar Cap Plasma Convection Measurements and Their Relevance to the Real-Time Modeling of the High Latitude Ionosphere," Proceedings of IEEE 87 Symposium on the Effect of the Ionosphere on Communication, Navigation, and Surveillance Systems, May 5-7, 1987.

Dennis, C. G., "A High Frequency Radio Technique for Measuring Plasma Drifts in the Ionosphere," Scientific Report No. 8, AFGL-TR-83-0262, Hanscom AFB, Massachusetts, July 1983. unknown

Gamache, R. R., W. T. Murphy and R. W. Reinisch, "Electron Density Profiles from Automatically Scaled Digital Ionograms. The ARTIST's Valley Solution," Scientific Report No. 1, AFGL-TR-86-0307, 1986. unknown

Gilbert, J. B. and R. W. Smith, "A Comparison Between the Automatic Ionogram Scaling System 'ARTIST' and the Standard Manual Method," submitted to Radio Science for publication in 1988.

Fotenauer, J. A., K. Bibl and R. W. Reinisch, "Direct Digital Graphics, The Display of Large Data Fields," Ionosonde Laboratory, pp. 96-101, September 1973.

Reinisch, R. W., "New Techniques in Ground-Based Ionospheric Sounding and Studies," Radio Science, 21, No. 3, pp. 331-341, May-June 1986.

Reinisch, R. W. and Huang Xueqin, "Automatic Calculation of Electron Density Profiles from Digital Ionograms, 3. Processing of Horizontally Stratified Ionograms," Radio Science, 18, 3, pp. 477-492, May-June 1983.

Reinisch, R. W., N. Ahmad, K. Bibl, M. Buchau, F. Gorman, J. D. Jodogne, L. Reasy, J. Ming and J. Gilbert, "A Transmitting Digital HF Radio Link Experiment," Proceedings of the Ionospheric Effects Symposium, Effect of the Ionosphere on C³I Systems, Alexandria, Virginia, pp. 111-117, May 1-3, 1984.

Reinisch, R. W., J. Stefan and E. J. Weber, "Digital Ionosonde Observations of the Polar Cap F Region Convection," Physica Scripta, 32, pp. 371-377, 1987.

Adv. Space Res. Vol. 8, No. 4, pp. (4)5–(4)8, 1988
Printed in Great Britain. 0273-1177/88 $0.00 + .50

REAL-TIME ELECTRON DENSITY PROFILES FROM IONOGRAMS

Boris W. Reinisch,* Robert B. Gamache,* Huang Xueqin** and Lee F. Mellstrom*

*University of Lowell Center for Atmospheric Research, Lowell, MA 01854, U.S.A.
*Research Institute of Radiowave Propagation, P.O. Box 138, Zhuxiang, Henan, PRC
**Andrew Antennas, Innovation House, Technology Park, The Levels, S.A. 5095, Australia

INTRODUCTION

Sounding of the three dimensional electron distribution in the earth's ionosphere is a requirement for both the radio communications engineer and the geophysicist probing the ionosphere and its interaction with the overlying atmosphere in terms of radiation and particle inputs from the sun. Global coverage with adequate spatial and temporal resolution must be provided by any data base if it is to be useful for the modeler.

At the present time, one of the best global descriptions of the electron density is given by the International Reference Ionosphere IRI-79 [1]. The IRI model is based largely on observational data obtained with ionosondes, incoherent scatter radar, rockets and satellites. Amongst these techniques, the ionosonde observations provide the best global coverage and, in principle, the best time resolution. The disadvantages of the ground-based ionosonde technique are well known: (1) no information on the topside F region, (2) limited sounding for the lower D-region and the valley information between the E and F regions, and (3) ambiguous evaluation of electron density profiles from the ionograms. Nevertheless, the existence of some one hundred ionosonde stations providing more or less continuous day and night-time profiles establishes the ionosonde network as an important contributor to the electron density data base.

As a result of advances in the electronic components area and the micro-computer field, modern ionosondes are available today that remove the need for manual conversion of the ionograms into vertical electron density profiles. Reinisch [2] showed that modern ground-based ionosondes can supply the profiles in real time, overcoming one of the limitations of ionosondes. If complementary data from modern topside ionosondes were available we would have a very comprehensive data base. In 1970, Bent and Llewellyn [3] used analog Alouette topside ionogram data for the modeling of the topside F region. Today three or four modern ionosondes [4] flown on orbiting satellites could provide automatic topside profile information on a world-wide basis. Automatic scaling techniques for topside ionograms already exist [5], [6], and vertical profiles can be reconstructed in output coordinates from [7]. Although such modern topside sounders are considered for the early to mid-nineties, they are not available now, and this paper therefore concentrates on the growing network of modern ground-based ionosondes.

SOUNDING THROUGH AN ION GAS

Since the Digisonde 256 [8] is the only currently available ionosonde that computes electron density profiles in real time, we will base our discussion on this system. The Digisonde records ionograms (Figure 1) in which the vertical echoes with ordinary and extraordinary polarization are clearly identified [9]. It's station the SPREAD, a PC-AT microcomputer, scrutinizes the virtual height traces $h'(f)$ for the E and F regions [10] (Figure 2), and the digisonde parameters determine. The $h'(f)$ traces are checked for scaling ambiguity (Figure 3) before the real profiles (Figure 4) is produced and checked (Figure 5, see [10]). The difference with other ionosonde program units in SPREAD is will be discussed in the next section. The coefficients of the polynomial profile representation are sent to a data server (Figure 6), where they join all digital ionosonde stations are combined to create global ionospheric maps (Figure 7).

Figure 1 shows automatically scaled ionograms from a polar cap (Thule,

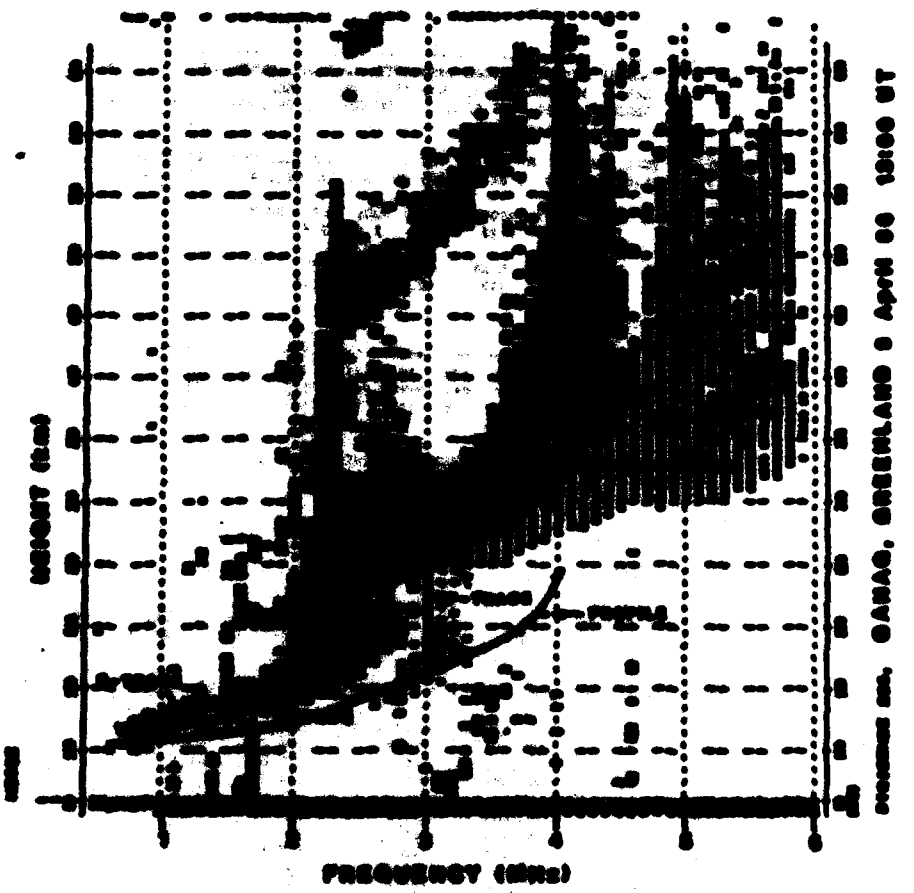

Figure 1. Polar cap ionogram

Greenland, 77.5°N, 69.2°W) station. The circles prepared of the ionogram was recorded at 15:00 UT (= 14:24 local mean) on 9 April 1958. The signal amplitude in units of 1 dB are shown as numbers 1, 2, ... If the echo height shift is positive, and as A, B, ... If the doppler is negative, signals with corresponding polarization are represented as X, and O(the) signals as Y(Z). Almost the discontinuity in leading edge of the E trace (called E-2 and the F2 trace (called F2-1) layer. The ordinary sounding profile, based on the NBAS method, is indicated as A. Some discussion of ionospheric sounding profiles under heavy ionized conditions, especially for polar cap are shown studies. For routine operation, the ionograms are not processed, and only the ionospheric parameters and the profile conditions are recorded (see Table 1).

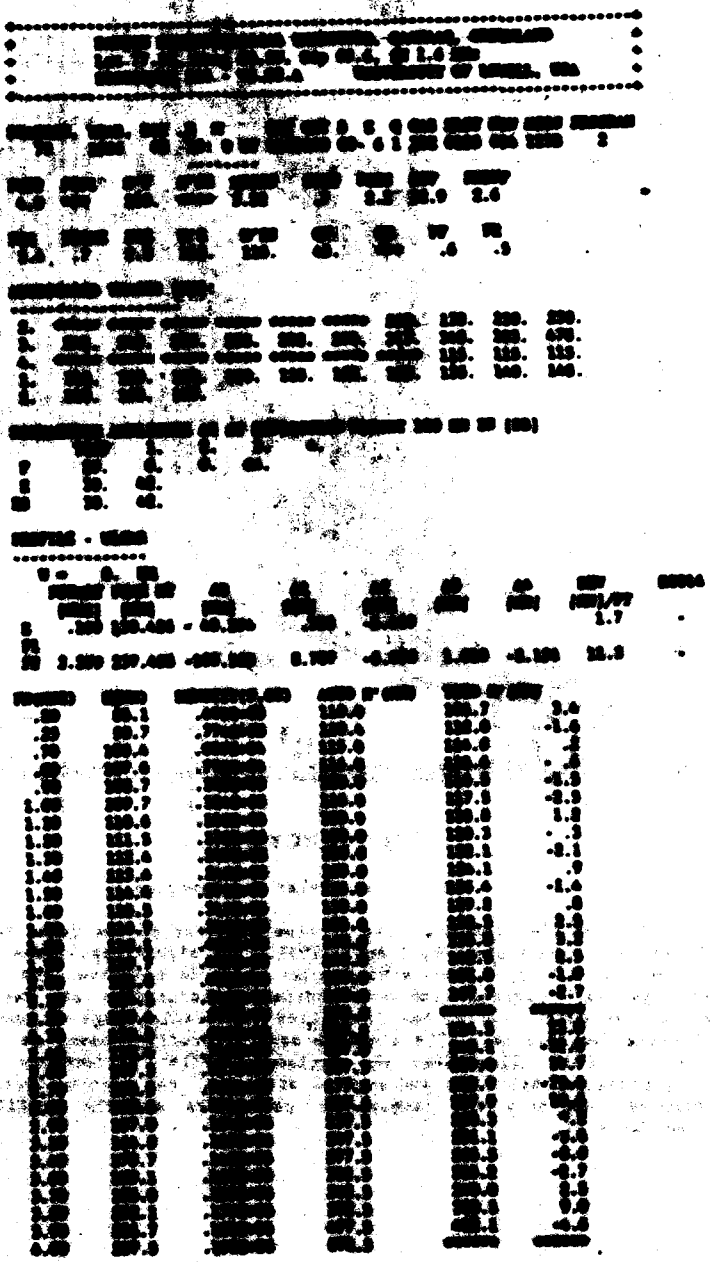

Table 1. [illegible]

[illegible]

$$z = z_0 + s^{1/n} \sum_{i=0}^{3} A_i T_i^*(\omega) \qquad (1)$$

where the A_i's are the coefficients of the polynomials, z_0 refers to the peak height of the layer and z_n given by z_0 - crest height - Σ_i A_i. The T_i^*'s are the shifted Chebyshev polynomials /15/, and s is

$$s = [\ln(z/z_{max})]/\ln[z_{max}/z_{min}]$$

Here z_{max} and z_{min} refer to the crest and and [illegible] of the respective layers, and z is the [illegible] coordinate. The factor $s^{1/n}$ multiplying the sum ensures an inflection always at the peak of the layer, where $s = 0$. The algorithm uses three terms ($i = 3$) for the E layer, five terms ($i = 5$) for the F1 layer when present, and five terms for the F2 layer. In order the A_i's' coefficients the algorithm accepts a variable which (2) also shows the E layer peak (Figure 2). τ is determined by a least squares fitting procedure /16/. This simplified approach contains that the original Rawlins-Huang method /16/, that included the search for a valley. Determination of the valley will be postponed until ARTIST provides the F layer [illegible].

The starting height of the profile is determined by the data, when making contact of [illegible] with [illegible]. The $y'(0)$ slope data (the E layer using the exp. and F using an elliptical model $f = 0$ by running a parabolic profile)

$$\zeta = \zeta(\mu \cdot (\tau))) \qquad (2)$$

with peak height the set coefficients μ, following the segments field, the corresponding virtual height using

$$\mu' = \frac{1}{\mu} \cdot \frac{\mu}{\mu} \cdot \frac{\mu}{\mu}$$

$$\mu = \mu \cdot \mu \qquad (3)$$

[illegible]

Rawlings's TRACE program is described in /16/. In the real time environment only

these codes which provide simple polynomial fits to each layer are useful. One of the [illegible] so that it can be used in ARTIST for real time [illegible] Code [illegible] is a simple polynomial fit [illegible] between the E and F regions [illegible] which is [illegible] In Figure 3, width W and depth D of the valley are listed as [illegible] less than [illegible] km. The effect of this shallow valley on the determination of the F region heights is expected to be very similar to that of the [illegible] plasma frequency [illegible] in the [illegible] model.

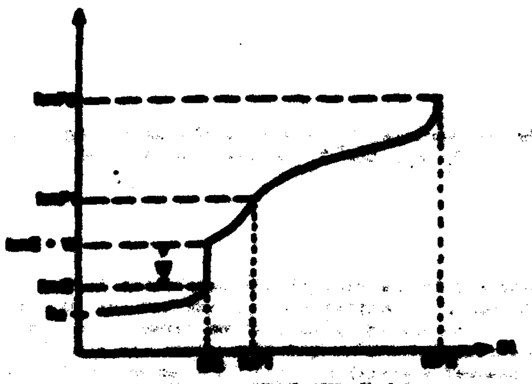

Figure 2

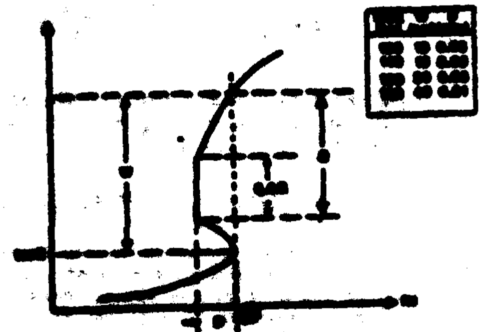

Figure 3

At the layer peaks, POLAN assumes a Chapman shape of the profile, while the ULCAR algorithm uses the modified polynomial approach [illegible] (see equation (1)) to fit the profile to the peak of the [illegible]. To study the effect of these different [illegible] mid-latitude station [illegible]. The same scaling [illegible] were used for both programs and the valley width was set equal to zero. The average height difference per ionogram was calculated, as well as the difference in the peak heights hmF2. Figure 4 compares the profiles obtained by the two different programs for a sample ionogram. The differences are consistently smaller than 3 km, as shown at the bottom of the figure. Taking the mean over the 170 ionograms, we find an average height difference of -3.8 km, and a mean peak height difference of -7.6 km. The minus sign indicates that the ULCAR routine gives slightly higher heights [illegible] while the POLAN peak height is slightly higher than the ULCAR peak. The difference is small considering the [illegible] resolution of 5 km.

We also compared the results of the two algorithms in their normal operational modes. The mean absolute height difference per ionogram is listed in Table 2 for 16 sample ionograms [illegible]. The code [illegible] is the standard ULCAR ARTIST code, and code [illegible] for semi-automatic analysis. [illegible] identified in Table 2 as [illegible] below the 3 km [illegible] km.

[illegible]

Electron density profiles derived automatically from digital ionograms provide a

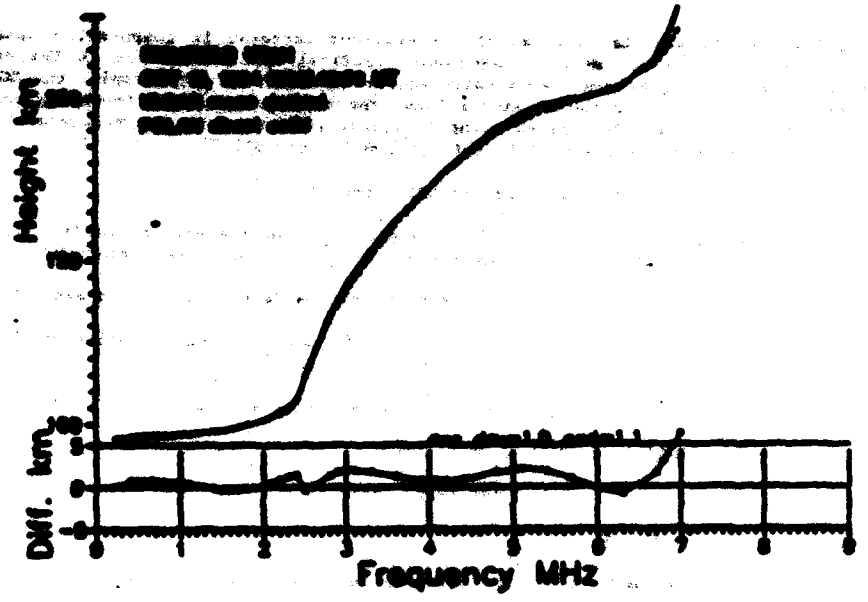

Profile Technique Comparison

Figure 4

Ionogram Day UT	foF2 MHz	Sum Width km	Alt. Mode <|Δh|> km	Alt. Mode σ km	Alt. Mode <|Δh|> km	Alt. Mode σ km	Amp. Mode <|Δh|> km	Amp. Mode σ km	Amp. Mode <|Δh|> km	Amp. Mode σ km
285.13:39	7.1	228.3	4.36	0.0	3.26	0.0	3.56	7.5	3.74	7.5
285.16:39	6.6	217.3	3.69	13.3	3.62	13.3	3.52	13.2	3.51	13.1
285.19:44	6.5	207.0	4.84	7.9	4.26	7.4	3.26	16.0	3.39	16.7
287.01:39	5.0	220.6	2.48	5.6	2.48	5.6	0.39	5.2	4.09	5.6
285.03:39	5.0	220.6	4.37	7.5	4.37	7.5	4.04	5.0	2.10	6.6
285.22:07	4.4	220.0	4.36	3.6	4.33	3.5	5.39	7.7	4.64	7.6
285.15:39	5.5	220.7	3.44	0.1	3.36	0.7	1.07	16.0	1.71	16.6
285.16:09	6.4	220.7	3.33	13.3	3.41	13.0	1.94	14.3	1.37	14.4
285.16:39	6.4	220.7	3.46	7.0	3.48	6.0	1.91	6.0	2.04	6.6
285.17:39	6.4	220.7	3.48	11.1	3.42	11.1	1.16	11.3	1.16	11.1
285.17:39	6.4	220.7	3.48	6.1	3.42	6.1	1.16	6.1	2.12	6.3
285.18:39	6.3	220.7	3.48	13.7	3.42	13.7	1.16	14.0	1.16	13.8
285.18:39	6.3	220.7	3.48	11.7	3.42	11.7	1.16	11.7	1.16	11.7
285.19:39	7.4	220.9	4.36	11.7	4.34	11.7	1.55	11.9	1.96	12.4

Table 2. Mean Absolute Height Difference for Normal Operational Modes

Validity tolerance for the scoring of simple models of the ionosphere. Simple models of the ionosphere were used for comparisons in which the errors in the resulting

calculations are disrupted because of the enormous increase in computation times which such models provide. One of the most important practical applications is in the calculation of Square Field ionograms and transmission loss curves. See, for example, the CCIR Supplement to Figure 252 /14/. For these calculations, the propagation codes involving reflections from the E and F layers are determined using an analytic model with parameters which depend on the previously scaled values of foE, foF1, foF2 and h'F,F2.

The model currently recommended by CCIR consists of:

A parabolic E layer below the height of maximum electron density, hmE, with semi-thickness ymE. hmE and ymE are set to 110 km and 30 km respectively.

A parabolic F1 layer with height of maximum density hmF1, and semi-thickness ymF1.

A linear increase of electron density between hmE and the point on the parabolic F1 layer where the plasma frequency is 1.7 foE.

The model parameter hmF2 is given by the empirical equations /14/, /17/:

$$hmF2 = 1490/(M(3000)F2 + dM) - 176 \quad (4)$$

with $$dM = 0.253/(R - 1.4) + 0.096 (M3K - 22)/150 \quad (5)$$

and $$R = foF2/foE, \text{ or } 1.7, \quad (6)$$

whichever is the larger. M3K is the 12-month smoothed sunspot number.

The term dM is an empirical correction term which takes into account the effects of underlying ionization not allowed for in the original Shimazaki /15/ formulation. Model estimates of hmF2 are usually considered to be correct to within 20 to 30 km /14/. Dubourg /16/ has described an improved model which uses a modified F1 layer shape and a more realistic E-F valley region, and has claimed that this model yields more accurate values of hmF2 than the Bradley-Dubourg /17/ model. Dubourg gives a revised formula for hmF2:

$$hmF2 = 1490\ T/(1 + dM) - 176 \quad (7)$$

where $$dM = 0.253/(R - 1.253) + 0.012 \quad (8)$$

and $$T = R\ [(0.0188\ R^2 + 1)/(1.2567\ R^2 - 1)]^{0.5} \quad (9)$$

The value of R is constrained to exceed 1.215.

Although, historically, Bradley and Dubourg /16/ have analyzed the differences between the foF2 and hmF2 values of both the CCIR and Shimazaki equations, according to the value of R (= foF2/foE) and to the value of the correction term dM.

Table 2 shows that the differences change from being exponentially positive for low R values, to being exponentially negative for high R values. Equation (4) indicates that the foF2 value can have only one hmF2 value. The second discrepancy is shown -3 km, but might reach a maximum of the values of zero in the different ranges of R. Dubourg specifies the high R value assumption as equation condition. For R ≥ 3, the discrepancy can be approximated as

$$dhmF2 = 22.5 - 8.2\ km. \quad (10)$$

Both the CCIR model and Dubourg model are very dependent on the sunspot number. The over-all accuracy of this Dubourg equation is very impressive for such a simple model.

[illegible]		[illegible]				Total %
-30	-25	1	1	19	13	6
-25	-20	1	0	11	20	8
-20	-15	0	1	20	20	13
-15	-10	4	6	16	17	8
-10	-5	4	24	17	8	13
-5	0	11	31	10	4	14
0	5	19	28	4	8	12
5	10	25	8	3	1	9
10	15	25	4	6	3	8
15	20	9	3	2	2	4
20	25	7	1	1	1	2
25	30	2	1	2	1	1
Number of Cases		200	243	94	180	

Table 3. Percentage distribution of discrepancies less than 30 km for all five stations, for four ranges of X.

The [illegible] high values of hmF2 given by the Bradley formula at night may be due to the model's neglect of underlying ionization. The effect of this underlying ionization was originally considered to be insignificant a decade or so ago, which it indeed was in comparison with the effects of the E and F1 layers during the day. However, the daytime models have been improved to the point where the nighttime errors are now the largest obtained.

An alternative explanation may lie in the variation with altitude of the F2 region scale height, which is not accounted for by the Bradley model.

DATA PRESENTATION AND ARCHIVING

Traditionally ionograms have been recorded on film and the frames projected for inspecting the ionograms. Today, modern ionosondes display the ionograms on inexpensive printers in real time (Figure 1). All store the [illegible] data in digital form on magnetic tape. Unfortunately, there is no general consensus as to what is essential. For routine operation it may suffice to tape record the [illegible] traces of the vertical echoes as well as the [illegible] parameters, and, since they are available, the coefficients of the electron density profile. This information can be [illegible] packed within one data block on tape. The Digisonde data blocks contain 4096 bytes, which means 5,000 ionograms can be recorded on a standard 2400 foot tape, or a little more than [illegible] weeks of data for quarter hourly ionograms. It is possible to [illegible] ionograms in one block, which would limit the number of tapes per year to three. For detailed ionospheric studies all ionogram data should be recorded on tape.

Magnetic tape storage of the true height profiles and the automatically scaled ionospheric data facilitates the analysis of the data in a very wide variety of ways. Two techniques have been developed at ULCAR for application with the data recorded from the Digisonde 256.

The first technique uses the F region true height electron density profiles that are calculated in real time and then stored on magnetic tape. A sequence of the profiles for one-day is presented in Figure 3. The three dimensions, height, time and electron density, are displayed as ordinate, abscissa, and a 16 level gray scale (Kapitson, /11/)

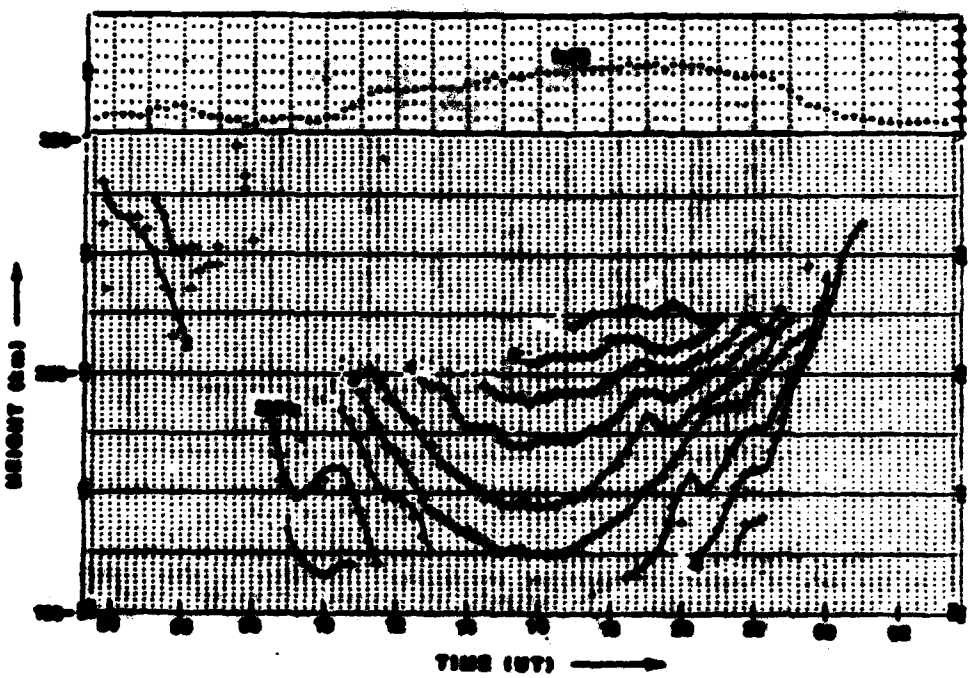

TIME (UT) ⟶

Electron Density Profiles 20-26 Feb 67 Argentia, Newfoundland
Plasma Frequency Contours with 0.5 MHz Intervals.

Figure 3

respectively. Iso-electron density contours result that are a function of time and height. Several features can be seen: the compression of the daytime F-layer to relatively low heights with short term variations that have a wave-like appearance and are likely associated with traveling ionospheric disturbances.

A second technique that we find finding useful for survey and study is a single sheet presentation of the day's complete, automated, ionograms. At a glance, one can easily detect events such as compression of sporadic E, sudden ionospheric disturbances, and the development of the main F-layer trough and its eventual exit. The single sheet compilations echo day-to-day comparisons easier than with film archived. They also enlarge dramatically the information content when compared to tables of scaled ionospheric parameters.

The examples shown here are but several of many that may prove useful for data presentation and archival. A key point is the recognition that magnetic media storage of ionospheric data enables computer aided analyses and presentations which heretofore were impossible or very labor intensive. The speedy turnaround, whether in space or on the ground, continues to produce important data for understanding ionospheric phenomena and for development of more realistic global ionospheric models. Additionally, the utility of these data is not limited by the storage media, and open new opportunities for tailored data presentation, archival and analysis consistent with the needs of a specific research study.

REFERENCES

1. K. Bowar, [illegible], World Data Center A (U.S.P.), Boulder, CO, USA (1961).
2. B. W. Reinisch, Radio Sci. 21, e6, 331-341 (1986).
3. R. B. Dent and S. K. Llewellyn, [illegible], Melbourne, FL, USA (1970).
4. E. E. Gotwols, D. E. Asbury, A. P. Mayer, K. Bibl, B. W. Reinisch and D. Lewis, in Proceedings IEEE, Ed. J. Goodman, Alexandria, VA, 634-643 (1981).
5. B. W. Reinisch and X. Huang, Radio Sci. 17, e2, 421-434 (1982).
6. S. Igi and K. Ailyo, Journal of the Radio Research Laboratory 33, e140, 169-183 (1986).
7. X. Huang and B. W. Reinisch, Radio Sci. 17, e4, 837-844 (1982).
8. B. W. Reinisch, Digisonde 256, in URSI Bulletin end.
9. K. Bibl and B. W. Reinisch, Radio Sci. 13, e3, 519-530 (1978).
10. B. W. Reinisch and X. Huang, Radio Sci. 18, e3, 477-492 (1983).
11. L. F. Hoffmann, Scientific Report No. 3, AFGL-TR-86-0058, ESD-TR-432/GRD (1986). ADA171328
12. J. E. Titheridge, [illegible], World Data Center A (U.S.P.), Boulder, CO (1985).
13. H. A. Snyder, Theorems Applied in Electrical Communication, Prentice Hall, New Jersey (1966).
14. B. W. Reinisch, K. Bibl, C. G. Deavin, R. R. Gamache, D. F. Kitrosser, S. W. Li, G. S. Sales and S.-H. Yeng, Final Report, AFGL-TR-87-0056, (1987). ADA192270
15. L. F. Hoffmann, Comput. Geosci. Elsev. 41, 343-348 (1979).
16. CCIR, Supplement to Report 252, International Radio Consultative Committee, International Telecommunication Union, Geneva, Switzerland (1980).
17. P. A. Bradley and J. E. Dudeney, J. Atmos. Terr. Phys., 35, 2131-2146 (1973).
18. T. Shimazaki, J. Radio Res. Labs., Japan, 2(7), 85-97 (1955).
19. J. E. Dudeney, J. Atmos. Terr. Phys., 45, 629-640 (1983).
20. L. F. Hoffmann, B. W. Reinisch and J. S. Yeng, Adv. in Space Research (1987).
21. J. Buresenda, K. Bibl and B. W. Reinisch, American Laboratory, 99-101, September 1971.

ACKNOWLEDGEMENT

The work of the University of Lowell authors was in part supported by the Air Force Geophysics Laboratory, Hanscom Air Force Base, Massachusetts.

Adv. Space Res. Vol. 5, No. 4, pp. [illegible], 1985
Printed in Great Britain.

[illegible]

LAY-FUNCTIONS FOR F2 PROFILES

L. Bossy,* R. R. Gamache** and B. W. Reinisch**

*Université Catholique de Louvain, B-1348 Louvain-la-Neuve, Belgium
**University of Lowell Center for Atmospheric Research, Lowell MA 01854, U.S.A.

INTRODUCTION

Bottom-type ionosondes /1/ calculate the vertical electron density profiles in real time providing a good data base for the global modeling of the ionospheric electron density distribution. The Digisonde 256 computes the profiles in form of coefficients for a polynomial representation /2/ for each of the layers. Then after publishing their results, Reinisch and Huang /3/ suggested the possibility of substituting LAY functions for the polynomial profile representations. In this paper we study the fitting of LAY functions profiles obtained in real time by Digisondes at Argentia, Newfoundland (47°N, 54°W), Richfield, Utah (39°N, 112°W) and Hamal, Brazil (3.7°S, 60°W). We use the technique proposed in /4/ to determine the LAY parameters BE and HE. Because of its efficiency this algorithm lends itself to real time processing.

FITTING OF LAY FUNCTIONS AND IMPLEMENTATION

The representation of the electron density profile of the F2 layer by a single LAY function is discussed. The LAY fitting used for this purpose has described in Reference 4. The advantage of the LAY function fit of the profile is that in general the entire F2 profile is well represented by one LAY function, defined by only four parameters foF2 (critical frequency), h_{max} (peak height), BE (height parameter) and HE (scale parameter) /4/. Other methods like the ULCAR Chebyshev polynomial representations require five coefficients plus the beginning and ending frequency of the layer. Titheridge's PROFILE true height analysis program /5/, in its parabolic mode (N), uses six coefficients per ramp plus the starting frequency and height; in the PROFILE polynomial mode used in the Digisonde (a 4th order polynomial), 11 parameters are needed to represent the F2 profile.

LAY function fitting was performed for over three thousand electron density height profiles which were calculated from ionograms with the POLAN method using a fourth order polynomial expansion of the F2 profile. The term of the LAY function always ensures a good fit at the layer peak, but it must be checked how far down in frequency the fit is acceptable. We defined error thresholds of 3 %, 5 %, and 10 % to determine the lower frequency limit of the fit. The 3 % threshold resulted in too narrow frequency intervals for which the fit is acceptable, and 10 % appears too coarse a measure. With a 5 % error, the LAY functions can describe almost the entire F2 region, so we decided to select the 5 % threshold for further analysis.

Our LAY analysis program computes and records the average absolute error per point in %, together with the number of frequency points and the threshold frequency foLAY. The values of foE, foF1 (when present), foF2, and the inflection point of the F2 profile are saved to study the steps of the LAY fits. From the parameters the ratios HE/h_{max} and (h_{max} - BE)/HE are calculated and stored. Since the profiles are available, we also determine the thickness δ from BE(0.5) - δ = h_{max} where N(0.5) is the height where the electron density is N = 0.5 N_{max} /6/. The δ thickness found for the profiles are compared with the value δ = 0.8 suggested by Rishbeth /6/.

Figure 1 is an example of the LAY function fits to a profile from Richfield, Utah, October 11, 1984 at 20:07 UT (20.07 LT). Here the previously LAY functions plotted in the dashing pattern as f_1 = 0.95foF2 and f_1 = 0.85foF2 and is shown along with the profile.

*Also Institute d'Astronomie Spatiale, B-1180, Brussels, Belgium

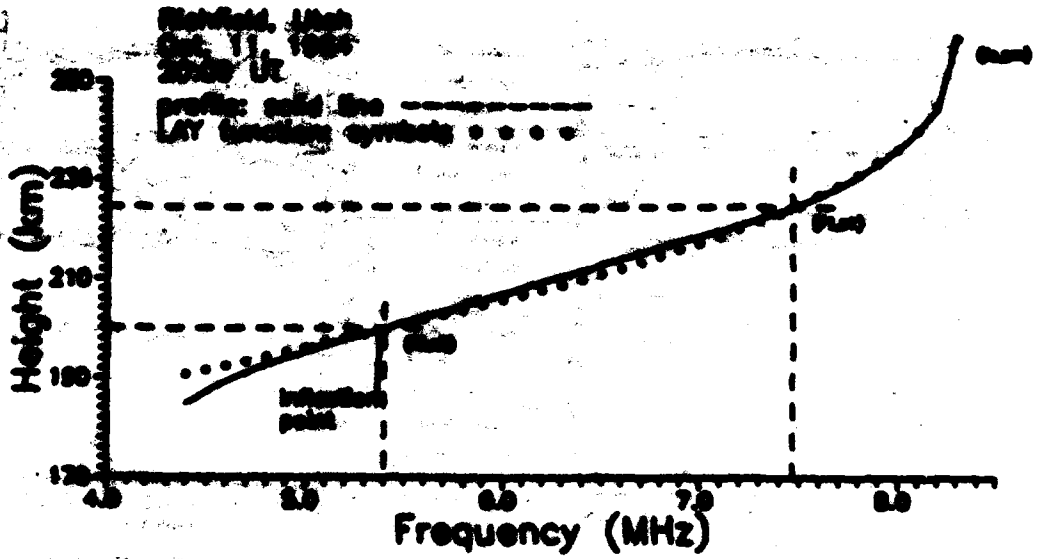

Figure 2. Fitting LAY function profile. The three selected points were (8.3 MHz, 205 km), (7.9 MHz, 196 km), and (5.4 MHz, 169 km). The LAY function approximates the F2 profile to frequencies well below the inflection point. foF1 for this ionogram is 4.3 MHz.

This fit has an average absolute error per point of 1.68 km with a 3 km maximum error, and agrees with the profile. The LAY parameters for this F2 profile are HX = 197 km and SC = 20.5 km.

ERRORS OF VALIDITY OF THE FIT

Our results show that most of the time the LAY functions, with 1 km maximum error, represent the whole F2 layer down to f = foE or foF1 during the day, and to the first sampled ionogram frequency during the night. The solid lines in Figure 3 represent the median values for Argentina, Uppsala and Grahamstown of the ratio foLAY/foF2. For Argentina, we analyzed profiles data for February/March, May/June and December/January 1958 (the upper three curves in Figure 3). The dashed lines represent the ratios foF1/foF2 during daytime when the F1 layer exists. The segments data should not be within 5% of foF1, i.e. not more than about 200 km above foF1. Whenever an F1 layer, detached or not, is present, the ionogram usually does not penetrate down to the lower F region. The horizontal lines at 70.7% for the segments curves indicate the level where the electron density N is half the maximum density of the layer.

SEASONAL VARIATIONS OF LAY PARAMETERS

For modeling purposes, it is desirable that the LAY parameters do not vary too rapidly as a function of time, and that deterministic predictor values exist for each season and time of day. Figure 4 shows the diurnal variations of the median values for X = HX/Hmax, expressed in percents. For Argentina, the median X lies generally between 70 and 80%, except during equinoctial seasons, when X drops down to 60%. The substantially larger data spread for

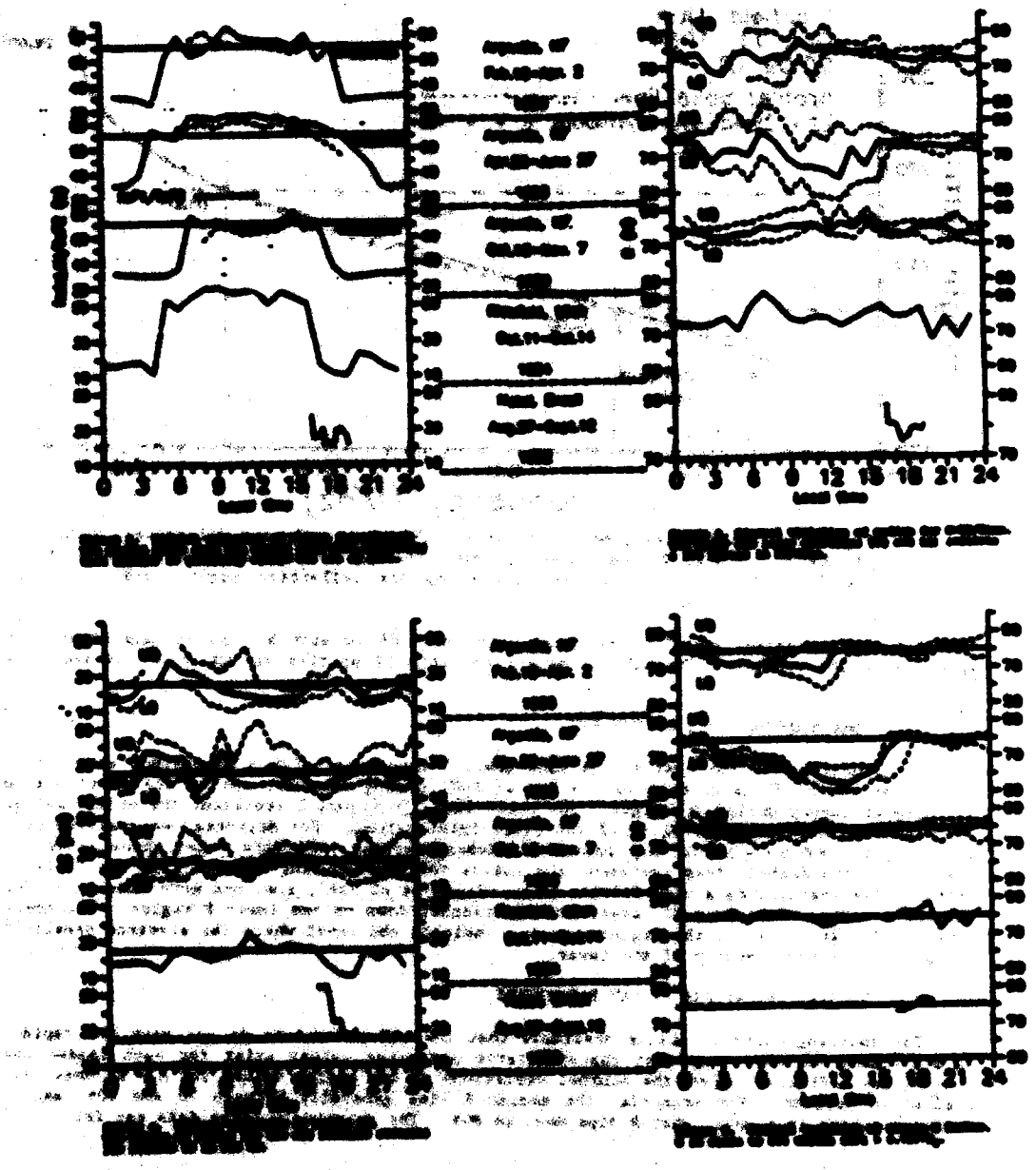

[illegible] allowed us determine the spread in B by calculating the upper and lower quartiles, called UQ and LQ respectively. It is interesting to see, that for periods of small diurnal variations the data spread is also small.

The relatively large B variations for Millstone are probably the result of the small data sample (only four days). For the equatorial station Ibadan, the available median B values fall in between 75 and 80%.

The median scale heights HS are generally confined to values between 25 km and 250 km, at least for Arecibo and Millstone. The spread in HS values for Arecibo, as indicated by the upper and lower quartiles, is at times considerable making it difficult to select a suitable HS for modeling purposes. The equatorial data for 1968 (high sunspot number) show a very different behavior, at least during the three hour period from 1600 to 1900 LT. HS decreases rapidly from 40 to 20 km. It would be necessary to study a longer equatorial data set to test the diurnal variation of HS at the equator.

Since all the data were available in the computer, we also calculated the Calspace G factor /6/. The median values for the three stations discussed for the LAY flevings are shown in Figure 5. For Jull, the G-value is close to 80% on all three occasions. However, substantial deviations exist in early spring and summer at Arecibo, when during daytime the median value dips below 60%. Of course, this is the effect of the F1 layer. In summer foF1 is consistently larger than 0.707 foF2, i.e. N(foF1) > 0.5 N_{max}, during the day (Figure 2), and the F1 layer shape factor C is well defined.

[illegible]

The F2 layer profiles can be expressed in terms of LAY functions with parameters HX/Hmax and HS that have a fairly small diurnal variation in their median values. Our studies could be expanded to express the entire E-F1-F2 profile as a linear combination of LAY functions, and investigate whether the LAY parameters HX/Hmax and HS still maintain a systematic behavior.

[illegible]

1. S. W. Reinisch, New Techniques in Ground-based Ionospheric Sounding and Studies, Radio Sci., 21, #3, 331-341 (1986).

2. S. W. Reinisch, B. R. Gamache, Z. Huang and L. F. Mckinnon, Real Time Electron Density Profiles from Ionograms, This Issue (1987).

3. S. W. Reinisch and Huang Xueqin, Automatic Calculation of Electron Density Profiles from Digital Ionograms. 3. Processing of Nonvertical Ionograms, Radio Sci., 18, #3, 477-492 (1983).

4. L. Scali, The Determination of LAY-Parameters for a Given Profile, Adv. in Space Res. Vol. 7, No. 6, p. 38 (1987).

5. J. E. Titheridge, Ionogram Analysis with the Generalized Program POLAN, Rept. UAG-93, World Data Center A (U.S.F.), Boulder, CO (1988).

6. T. L. Calspace, Implementation of a New Characteristics Parameter into the ISI Sub-Peak Electron Density Profile, Adv. Space Res., 2, No. 10, 101-104 (1983).

[illegible]

The work of the University of Lowell authors was in part supported by the Air Force Geophysics Laboratory, Hanscom Air Force Base, Massachusetts.